Ganglioside embedded in reconstituted lipoprotein binds cholera toxin with elevated affinity[S]

Daniel A. Bricarello,* Emily J. Mills,* Jitka Petrlova,† John C. Voss,† and Atul N. Parikh[1,*]

Departments of Applied Science* and Biochemistry and Molecular Medicine,† University of California, Davis, CA 95616

Abstract **The ability to exogenously present cell-surface receptors in high-affinity conformations in a synthetic system offers an opportunity to provide host cells with protection from pathogenic toxins. This strategy requires improvement of the synthetic receptor binding affinity against its native counterpart, particularly with polyvalent toxins where clustering of membrane receptors can hinder binding. Here we demonstrate that reconstituted lipoprotein, nanometer-sized discoidal lipid bilayers bounded by apolipoprotein and functionalized by incorporation of pathogen receptors, provides a means to enhance toxin-receptor binding through molecular-level control over the receptor microenvironment (specifically, its rigidity, composition, and heterogeneity). Using a Foerster Resonance Energy Transfer (FRET)-based assay, we found that reconstituted lipoprotein incorporating low concentrations of ganglioside monosialotetrahexosylganglioside (GM1) binds polymeric cholera toxin with significantly higher affinity than liposomes or supported lipid bilayers, most likely a result of the enhanced control over receptor clustering provided by the lipoprotein platform. Using wide-area epifluorescence, we found that this enhanced binding capacity can be effectively utilized to divert cholera toxin away from populations of healthy mammalian cells. In summary, we found that reconstitutions of high-density lipoprotein can be engineered to include specific pathogen receptors; that their pathogen binding affinity is altered, presumably due to attenuation of receptor aggregation; and that these assemblies are effective at protecting cells from biological toxins.**—Bricarello, D. A., E. J. Mills, J. Petrlova, J. C. Voss, and A. N. Parikh. **Ganglioside embedded in reconstituted lipoprotein binds cholera toxin with elevated affinity.** ***J. Lipid Res.*** **2010.** 51: **2731–2738.**

Supplementary key words reconstituted high-density lipoprotein • GM1 • pathogen • binding affinity • inhibition of toxin binding

As part of its innate immune system, the human body often presents cell-surface receptors in an extracellular environment as "decoys" to protect its native cells from attacks by pathogenic toxins (1, 2). Central to this biological strategy is the enhanced capacity of cellular receptors presented as decoys to outcompete native toxin receptors on host cells. An extraordinarily powerful example of this native defense strategy is provided by human milk. The lipid shell of milk fat globules contains many membrane-associated glycoproteins (and enzymes) that are selectively acquired from the plasma membrane during secretion. Presentation of these glycoconjugates and other oligosaccharides in this modified-membrane environment is thought to protect the nursing infant by offering an alternate pathogen binding site (3–5). From an evolutionary perspective, this type of molecular lure is important in the reproductive process, as it has the capacity to prevent enteropathogens from attaching to potential host cells in newborns. Successfully mimicking this protective mechanism could lead to improved techniques to combat infectious disease. Synthetic constructs that contain potent receptors could mitigate pathogen attacks on host cells and establish the foundation for an interventional therapy against infection (6).

Our strategy focuses on reconstituted lipoprotein, nanometer-sized discoidal lipid bilayers of arbitrary composition bounded by apolipoprotein, to construct a versatile, biocompatible, and stable platform that appropriately partitions pathogen-binding receptors into membrane-like environments. The selection of reconstituted high-density lipoprotein (rHDL) as a biosynthetic decoy is based on several factors. First, rHDLs are essentially endogenous

This study was supported in part by US Department of Energy Grant DE-FG02-04ER46173 (Biomolecular Materials, Division of Materials Science & Engineering) and by the Nanomedicine Development Centers of the National Institutes of Health Roadmap Initiative. Its contents are solely the responsibility of the authors and do not necessarily represent the official views of the National Institutes of Health or other granting agencies.

Manuscript received 5 April 2010 and in revised form 14 May 2010.

Published, JLR Papers in Press, May 14, 2010
DOI 10.1194/jlr.M007401

Abbreviations: ApoA-I, apolipoprotein A-I; CH, cholesterol; CTB, cholera toxin subunit B; DPH, 1,6-diphenyl-1,3,5-hexatriene; FITC, fluorescein-isothiocyanate; FRET, Foerster Resonant Energy Transfer; GM1, monosialotetrahexosylganglioside; NBD, N-(7-nitrobenz-2-oxa-1,3-diazol-4-yl); rHDL, reconstituted high-density lipoprotein; RPE, retinal pigment epithelium; TR, Texas red.

[1] To whom correspondence should be addressed.
e-mail: anparikh@ucdavis.edu

[S] The online version of this article (available at http://www.jlr.org) contains supplementary data.

particles and likely to be fully biocompatible. Native lipoproteins, in their nascent form, are composed of a nanometer-scale (10–20 nm) discoidal patch of lipid bilayer bounded by wild-type apolipoprotein (**Fig. 1**). The reconstituted version self-assembles after simply combining some or all of the constituent components under appropriate conditions (7–9). Second, the lipid bilayer environment of their core allows incorporation of membrane receptors (10) a priori during their reconstitution. Previous studies document successful inclusion of a wide range of membrane proteins and receptors, including proton pumps (11), membrane-associating enzymes (12, 13), and signaling molecules (10, 14). Third, because many pathogen interactions with cellular receptors are polyvalent in nature, the small nanoscale dimensions of rHDL make it unique in reducing clustering and increasing the probability of monovalent interactions. Specifically, the contiguous lipid bilayer provided by this construct is only 10–20 nm in diameter (8) and, with proper construction, can be engineered to contain just a few receptors, potentially reducing the average number of receptors per structure by a factor of 10^2 (**Table 1**). Fourth, the rHDL platform compartmentalizes the membrane into discrete nanoscale particles. Thus, after the initial attachment of ligand, recruitment and cross-linking of additional membrane-bound receptors is hindered by their disperse distribution across multiple particles. And finally, recombinant lipoproteins or their synthetic analogs have been tested in a variety of studies as potential therapeutic treatments (15–19), thus extending their relevance to our current efforts.

To perform a comparative analysis of the effects of the membrane-scaffold on receptor-ligand interactions, a well-characterized system with high specificity is needed. The interaction of cholera toxin (an AB_5 protein ligand) with membrane-bound monosialoganglioside GM1 (a glycolipid receptor) is an excellent candidate. Naturally-occurring GM1 is a native receptor for cholera toxin. It is thought to localize in highly ordered, cholesterol-enriched specialized lipid microdomains (called "rafts") in the extracellular leaflet of the plasma membrane (20). Binding is multivalent in this receptor-ligand pair as the protein toxin has a pentameric configuration of the binding epitope (i.e., five B-subunits) (21). In host cells, the protein toxin exploits the translational mobility of ganglioside by attaching to multiple receptors, disrupting lipid organization, and eventually penetrating the plasma membrane (22). At first glance, it would appear that an effective toxin decoy could be constructed by simply equipping a synthetic lipid vesicle (or comparable lipidic mesophases) with an exaggerated GM1 concentration. However, closer examination reveals additional factors that render this strategy ineffective. The ligand-receptor interaction involves attachment of the toxin to the ganglioside pentasaccharide moiety via hydrogen bonds (21, 23), which can also form between GM1 headgroups. These headgroup-to-headgroup links result in preferential association between GM1 molecules within the lipid bilayer, forming clusters visible in Transmission Electron Microscopy (TEM) and Atomic Force Microscopy (AFM) images. (24, 25). Such preclustering of GM1 limits its availability for attachment to the invading protein toxin. As a consequence, simply increasing receptor concentration is not sufficient. Engineering the membrane structure to limit receptor clustering is necessary to enhance toxin binding.

TABLE 1. Results of linear regressions fit to both vesicle and rHDL systems with varying concentrations of GM1

	GM1 (mol%)	Association Constant $(\mu M)^{-1}$	R^2	Receptors per Particle
Vesicles	0.25	8.8 ± 2.4	0.989	148
	0.50	6.9 ± 1.8	0.993	295
	1.0	6.2 ± 1.6	0.998	590
	Raft[a]	4.1 ± 1.1	0.994	590
	5.0	11 ± 0.6	0.997	2950
rHDL	0.25	24 ± 4.3	0.995	0.5
	0.50	27 ± 6.2	0.979	1
	1.0	27 ± 5.4	0.979	2
	5.0	13 ± 3.0	0.995	10

Association constant has units 10^6 M^{-1} and is given as the mean average of duplicate runs with uncertainty equal to the standard deviation. The R^2 value of each fit is reported along with the average number of GM1 molecules per lipid structure. Abbreviations: DOPC, 1,2-dioleoyl-sn-glycero-3-phosphocholine; GM1, monosialotetrahexosylganglioside; rHDL, reconstituted high-density lipoprotein.

[a]1 mol% GM1 added to vesicles constructed of equimolar concentrations of DOPC:SM:cholesterol(CH).

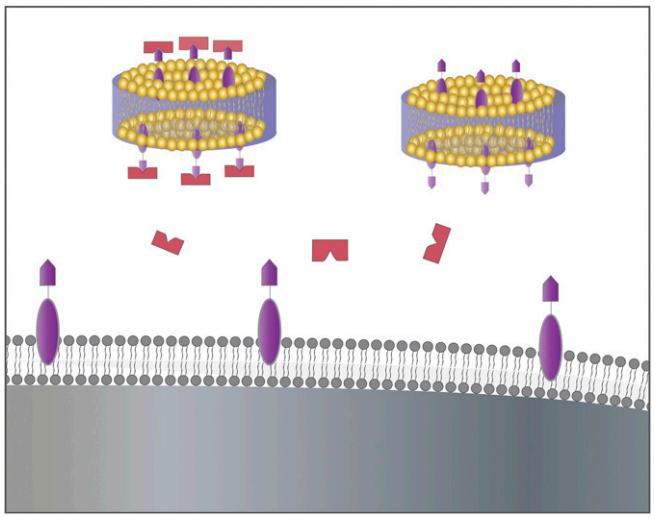

Fig. 1. Potential protective mechanism. Polyvalent ligands (red) binding to both receptors (purple) embedded in lipoprotein (yellow) and nonclustered receptors within a fluid membrane (gray). Depicted from left to right in the fluid membrane are incidents of ligand-receptor monovalent binding, receptor clustering, and receptor cross-linking.

MATERIALS AND METHODS

Materials

1,2-Dimyristoyl-sn-glycero-3-phosphocholine (DMPC), 1,2-dioleoyl-sn-glycero-3-phosphocholine (DOPC), sphingomyelin, cholesterol (ovine wool)(>98%), and GM1 ganglioside (brain, ovine, ammonium salt) were obtained from Avanti Polar Lipids (Alabaster, AL). 1,6-Diphenyl-1,3,5-hexatriene (DPH), Texas Red 1,2-dihexadecanoyl-sn-glycero-3-phosphoethanolamine, tri-

ethyl-ammonium salt (TR-DHPE), N-(7-nitrobenz-2-oxa-1,3-diazol-4-yl)-1,2-dihexadecanoyl-sn-glycero-3-phosphoethanolamine, triethyl-ammonium salt (NBD-PE), along with Alexa594-labeled cholera toxin subunit (CTB) were purchased from Invitrogen (Carlsbad, CA). Fluorescein-isothiocyanate (FITC)-labeled cholera toxin subunit B was obtained from Sigma Aldrich (Milwaukee, WI). All lipids were suspended and stored in chloroform or chloroform/alcohol mixture in the freezer (−20°C) until use. DPH was suspended in ethanol at 50 μM. All chemicals were used without further purification. Organic-free deionized water of high resistivity (18.2 MΩ-cm) was obtained by processing water first through a reverse-osmosis deionization unit and then a Millipore Synthesis water filtration unit (Billerica, MA). Phosphate-buffered saline (pH = 7.4) was obtained from Gibco-Life Technology (Rockville, MD) and used as buffer medium.

Expression and purification of recombinant human apoA-I

Human apolipoprotein A-I (apoA-I) was expressed in bacterial cells using the pET-20b-based (Novagen, Inc., Madison, WI) vector pNFXex with attached His Tag (26), kindly provided by Dr. M. Oda (CHORI, Oakland, CA). The pNFXex plasmid was transferred into the *Escherichia coli* stain BL21 Star (DE3) cells (Invitrogen) and cultivated at 37°C in LB medium with 50 μg/ml of ampicillin. Protein expression was induced for 3–4 h following the addition of 0.5 mM IPTG. ApoA-I was purified from the soluble fraction of the cells using His-Trap-Nickel-chelating (GE Biosciences, NJ) column as described previously (27). Briefly, the soluble extract was loaded and washed using a mobile phase of PBS (pH 7.4) with 3 M guanidine•HCl. The apoA-I was then washed in PBS (pH 7.4) containing 100 mM imidazole, and then eluted with PBS containing 500 mM imidazole. Imidazole was removed from the protein sample by using Bio spin columns (Bio-Rad) equilibrated with PBS (pH 7.4).

Preparation of vesicles

Small unilamellar vesicles (SUV) were prepared using standard vesicle extrusion methods. Typically, DMPC and GM1 suspended in chloroform were mixed in a glass vial. The solvent was evaporated under a stream of nitrogen and subsequently evacuated for at least 1 h in a vacuum desiccator. The dried mixture was then suspended in PBS heated to 35°C. The total lipid concentration was 1 mg/ml. The desired amount of hydrated aqueous solution was then sonicated and passed through an Avanti Mini-Extruder (Avanti, Alabaster, AL) using 100 nm polycarbonate membrane filters (Avanti) 21 times at 35°C. Vesicles were used immediately following extrusion.

Reconstitution of GM1-laden high-density lipoprotein

The 100 nm DMPC/GM1 vesicles were mixed with wild-type apoA-I (0.1–0.25 mg/ml) at an 80:1 lipid-to-protein molar ratio and incubated overnight (15–18 h) at 24°C. Samples prepared in this manner were used the following morning.

Fluorescence spectroscopy

Spectroscopic analysis was performed with a Perkin-Elmer LS 55 Fluorescence Spectrometer (Waltham, MA). The donor probe used in the Foerster Resonant Energy Transfer (FRET) quenching assays was 70 μM DPH in ethanol, which only fluoresces in a hydrophobic environment, added at a 200:7 lipid-to-probe ratio. After a 30 min delay to allow DPH partitioning, FITC-labeled cholera toxin subunit B was added in 5 μg aliquots to the GM1-laden lipid solution and allowed to bind for 5 min. Control analyses indicate this period of time is sufficient for the reaction to equilibrate. Subsequent binding of cholera toxin was then tracked by monitoring the reduction in DPH emission due to Forster Resonant Energy Transfer. FITC and DPH share significant spectral overlap (**Fig. 2A**), allowing FRET over a Foerster distance of 4.5 nm (28). GM1 and CTB concentrations were selected to span a range of GM1/CTB ratios from 20 to 1. This

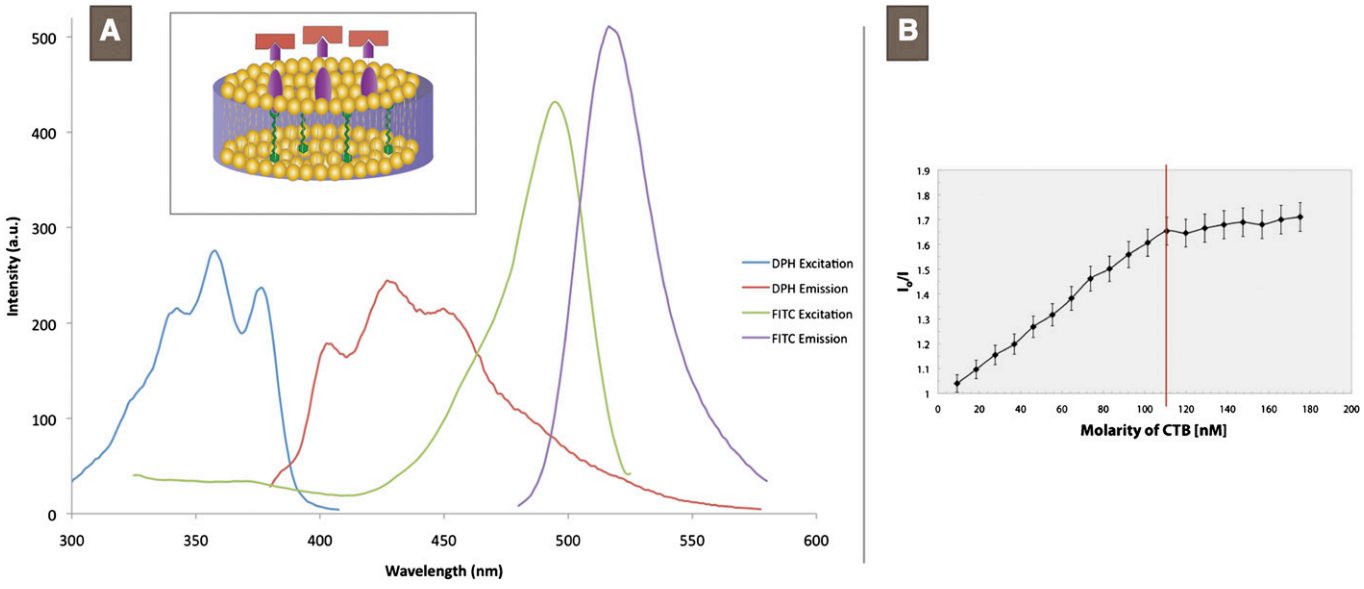

Fig. 2. Characterization of FRET pair and toxin-quencher titration. A: Excitation and emission spectra of DPH and FITC-CTB. Intensity of each spectrum is not to scale. Inset: schematic representation of DPH (green) embedded in the hydrophobic core of the lipoprotein (yellow) and its proximity to a receptor (purple) and fluorescently-labeled pentavalent ligand (red). B: Stern-Volmer plot of GM1-CTB binding for DMPC vesicles containing 1.0 mol% GM1. The independent axis is molarity of CTB (nM) and the dependent axis is the inverse normalized donor fluorescence (I_o/I). Error bars are derived from instrument error. The entire collection of S-V plots are available in the supplementary data. CTB, cholera toxin subunit B; DMPC, 1,2-dimyristoyl-sn-glycero-3-phosphocholine; DPH, diphenylhexatriene; FITC, fluorescein-isothiocyanate; FRET, Foerster Resonant Energy Transfer; GM1, monosialotetrahexosylganglioside.

range allowed identification of the saturation point to ensure only data collected during binding was included in the analysis. All spectroscopic analyses were performed at a temperature of 37°C in phosphate-buffered saline at pH 7.4.

Calculation of binding constants

The Stern-Volmer equation describes the relationship between the measured donor emission *I* and quencher concentration *[Q]*:

$$\frac{I}{I_o} = 1 + K_S[Q]$$

where K_S is the quenching constant. By plotting these values (*I* versus *[Q]*) and fitting a trend line (calculated using Microsoft Excel without fitting to expected boundary conditions), the value of K_S can be calculated. This constant is determined (29) from the concentrations of the fluorophore *[F]*, quencher *[Q]*, and fluorophore-quencher complex *[FQ]*:

$$K_S = \frac{[FQ]}{[F][Q]} = \frac{[CTB]_{bound}}{[DPH] \times [CTB]_{free}}$$

This relationship is, of course, the equilibrium association constant k_a for the reaction $F + Q \rightarrow FQ$ or $CTB + DPH \rightarrow CTB_{bound}$. The concentration of DPH (fluorescent donor) is identical in all samples so it is not equal to the GM1 (binding receptor) concentration of each; the quenching constant determined here is not equivalent to the traditional definition of binding affinity (which, due to the polyvalency, is quite complex). In this experiment, because the toxin can only quench one donor molecule per binding event (due to the quantized nature of the energy transfer process), the calculated equilibrium constant actually describes the interaction of CTB with the lipid structure. Thus, an effective or apparent equilibrium binding constant is determined, independent of GM1 concentration. This fluorescent quenching method is similar to fluorescent methods used previously (25, 30, 31), with the exception that quenching is used to quantify binding in bulk solution. We were unable to identify any potential cause of fluctuation in FRET efficiency as a function of GM1 concentration or lipid-structure type, so no modifications were made to the mathematical relation (see supplementary data for additional qualification of this method).

RPE cell culture and rHDL incubation

Human retinal pigment epithelium (ARPE-19) cells were obtained from ATCC (CRL-2302; ATCC, Manassas, VA). Cells were cultured at 37°C in the presence of 5% CO_2 in DMEM/F12 basal medium supplemented with 10% (v/v) fetal bovine serum, 1% (v/v) 200 mM L-glutamine, 1% (v/v) 10,000 units penicillin/streptomycin, 0.1% (v/v) 50 mg/ml gentamicin (Invitrogen, Carlsbad, CA), 0.2% (v/v) normicin (Invivogen, San Diego, CA), and 1.25 g/l cell culture grade $NaHCO_3$. Cells were grown in 75 cm^2 cell culture flasks (NUNC #156499). Total passage number is less than 30. Cells were then subcultured onto 5 ml petri dishes and allowed to grow for 7–10 days until confluent. This cell line was chosen as it is known to contain GM1 (32) and grows as adherent cells, which are convenient for microscopy. To test for rHDL-cell interactions, 50 µl of 1 mg/ml vesicles or rHDL was prepared with 2 mol% Texas Red-DHPE and allowed to incubate in PBS-submerged cells for 2 h, then rinsed. Cell incubations were performed at elevated temperatures to ensure DMPC was in the fluid phase.

rHDL, CTB, and cell incubations

To test for rHDL-cell interactions, cells were transferred from their growth medium to laboratory petri dishes containing PBS, where all incubations were performed for 2 h at 37°C. Additional controls were also performed to determine if the presence of GM1 within the HDL plays a role in preventing CTB interaction with cells. Other samples were incubated with Alexa594-CTB and rHDL containing no GM1 (see supplementary data). Another set was incubated in 20 µl of 1 mg/ml FITC-CTB alone (data shown in Fig. 5). The final fraction of cells were incubated with 20 µl of 1 mg/ml Alexa594-CTB concurrently with GM1-laden, NBD-labeled (DMPC doped with 3 mol% NBD-PE) lipid complexes at a 1:1 GM1-to-CTB ratio. The lipid complexes employed included vesicles containing 1 mol% GM1, vesicles containing 10 mol% GM1, rHDL containing 1 mol% GM1, and rHDL containing 10 mol% GM1. Unbound particles were removed before imaging by rinsing with PBS. The 1:1 GM1-to-CTB ratio is necessary as it ensures the amount of decoy GM1 added does not overwhelmingly exceed that present in RPE cells.

Epifluorescence microscopy

A Nikon eclipse TE2000-S inverted fluorescence microscope (Technical Instruments, Burlingame, CA), equipped with Retiga-1300 CCD camera (Technical Instruments) and an Hg lamp as the light source, was used to visualize all fluorescent samples. Images were stored and processed using simple PCI software (Compix, Inc., Cranberry Township, PA) augmented with a quantitative dynamic intensity analysis module. Fluorescence images were taken with the Texas Red filter set for both TR as well as Alexa-labeled CTB particles. Excitation and emission maxima for the TR are 583/601 nm and for Alexa Fluor are 578/603 nm. NBD-labeled particles were imaged with the NBD filter set, which has excitation and emission maxima of 465/537 nm. Phase-contrast images of single-layered RPE cells obtained under bright-field illumination were aligned and merged with those from the fluorescence channel(s). Visual inspection of these layered images shows the magnitude of CTB-cell interactions. The salient features are overlapping patterns of identical shape and shading which indicate close association of toxin and cells. Using these microscopy techniques, it was possible to detect the adherence of fluorescently tagged cholera toxin to cells and build a qualitative comparison of the degree of binding. All samples intended for microscopic analyses were incubated at a temperature of 37°C in PBS at pH 7.4.

UV patterning and surface-supported sample preparation

A binary pattern of rHDL and a supported DMPC bilayer was constructed by first adsorbing 40 µL of 2 mg/ml rHDL solution containing 1 mol% GM1 to a piranha-etch cleaned glass cover slip for 30 min. By illuminating the sample with deep UV radiation through a quartz-chrome mask with 50 µm opaque squares, rHDL was selectively removed from the grid-like region (8, 33). Low-wavelength UV radiation produces short-lived reactive oxygen species in the immediate vicinity of the surface film, resulting in the chemical degradation of organic material. After resuspending the patterned substrate in PBS, 80 µL of 2 mg/ml water-filled 100 nm DMPC vesicles also containing 1 mol% GM1 was added and allowed to fuse in the UV-exposed region. Finally 30 µL of 0.2 mg/ml Alexa594-CTB was added based upon a 2:1 ratio with the amount of GM1 added to the substrate (assuming 40 µL of 2 mg/ml solution results in complete surface coverage). Control experiments without GM1 show little fluorescence, suggesting very little nonspecific adsorption of CTB (data not shown). Acquired fluorescence images were line scanned using ImageJ. Intensity values were normalized to background levels present in the region where fluorophores were mechanically removed from the substrate.

RESULTS AND DISCUSSION

A fluorescence-microscopy-based assay comparing binding in GM1-decorated supported bilayers with substrate-immobilized rHDL (**Fig. 3**) provides preliminary support for our approach. Subsequent vesicle fusion of the same lipid composition present in the rHDL completes the preparation of the sample. From the line scan across both regions of rHDL (inside squares) and fluid bilayer (outside squares), there is a 2- to 3-fold increase in fluorescence due to CTB binding in the rHDL region. These initial findings suggest that GM1 binds a greater amount of CTB when it is incorporated in rHDL. Furthermore, the saturating concentration of CTB ensures that the resulting fluorescence can be interpreted as an improvement in the association constant (i.e., more CTB-GM1 bonds are formed per GM1 molecule).

Stern-Volmer (29) analysis of FRET-quenching data collected from a self-consistent set of systematically varied, physiologically relevant GM1 concentrations (0.25, 0.50, 1.0, and 5 mol%) in vesicular and rHDL configurations are summarized in Table 1. By embedding a donor fluorophore in the lipid bilayer (DPH) and attaching a fluorescent acceptor (FITC) to the protein toxin, association of CTB with the lipid surface can be tracked by monitoring the decrease in donor emission (Fig. 2B). Note that this technique allows calculation of an apparent or effective equilibrium constant only and does not account for mono- or polyvalency (see supplementary data for additional information). Table 1 also presents estimates for the number of receptor molecules per contiguous mesophase, namely, vesicle or rHDL, for comparison. There are at least two noteworthy features in these data, which are discussed below.

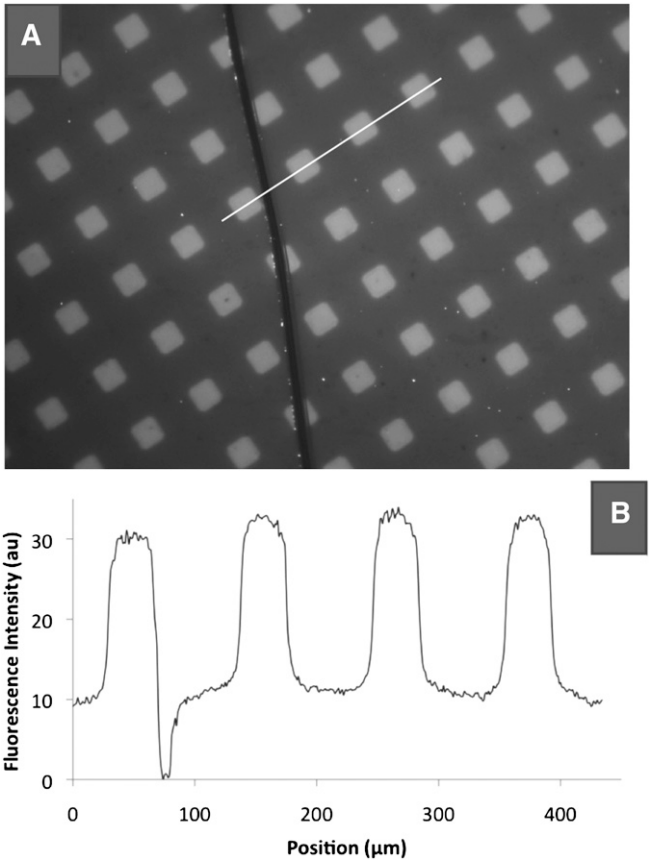

Fig. 3. CTB-GM1 binding in surface-supported membranes. A: UV patterning enables a side-by-side comparison of Texas Red-labeled cholera toxin binding to 1 mol% GM1 supported in a fluid DMPC bilayer (outside squares) versus rHDL supports (inside squares). B: A plot of the fluorescence intensity along the line shown, indicates a 2- to 3-fold increase between the region inside and outside of the squares. CTB, cholera toxin subunit B; DMPC, 1,2-dimyristoyl-sn-glycero-3-phosphocholine; GM1, monosialotetrahexosylganglioside.

First, for vesicular configurations, the effective binding constants are in a narrow range of $4–11 \times 10^6\ M^{-1}$ These values are in good general agreement with previous studies where comparable vesicular or planar bilayer configurations were employed (31, 34). Although it is notable that depending on the exact geometry of the experiment and specific types of receptor and ligand components used (e.g., soluble versus insoluble, labeled versus unlabeled, planar versus spherical), differences of two to three orders of magnitude in binding affinities have been observed (34).

Second, a closer inspection reveals that for increasing receptor concentration (or number of receptors per single vesicle), the binding constants display a small but unmistakable drop. This decrease is consistent with, but does not independently establish that the aforementioned GM1 clustering may inhibit CTB binding for elevated receptor concentrations.

Most importantly, however, it is immediately observable from our data that binding to rHDL is 3- to 5-fold higher than for corresponding compositions in vesicles. A recent study by Borch et al. (35) has shown the binding of cholera toxin to synthetic lipoprotein immobilized on active planar surface plasmon resonance (SPR) surfaces. Consistent with our findings, they note a difference in the equilibrium constant of cholera toxin binding to lipoprotein versus planar-supported bilayers deposited on SPR surfaces. Our results confirm their proposition and the influence of the membrane microenvironment on receptor-ligand interactions. This difference in binding affinities for identical GM1 concentrations in vesicular and rHDL environments can be ascribed to three primary effects of the microenvironment on toxin binding. First, GM1 within laterally unconstrained phospholipid bilayers (e.g., vesicles) is known to exhibit a strong tendency for lateral aggregation. These self-segregating clusters are known to be present in free bilayers at GM1 concentrations as small as 0.1 mol% (25). As discussed above, this lateral clustering can be expected to decrease the amount of GM1 available for binding. The compact lipid platform of rHDL, however, significantly restrains receptor aggregation. The size of rHDL is significantly smaller than the 20–30 nm GM1 cluster diameter, previously reported in AFM scans of supported bilayers, thus restricting the largest possible cluster size (25). Second, following initial monovalent attachment of CTB, binding of additional receptors is hindered due to

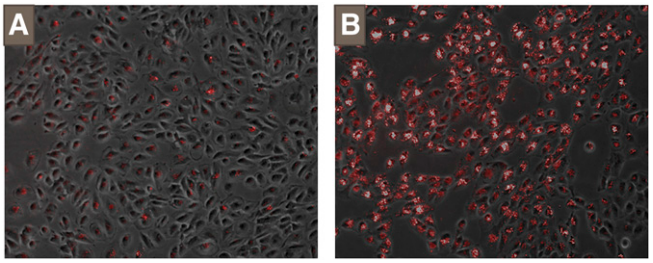

Fig. 4. Interaction of cells with vesicles and rHDL separately. Equal concentrations of fluorescently-labeled lipid particles are incubated for 4 h with RPE cells. POPC 100 nm diameter unilamellar vesicles with 2 mol% Texas Red-DHPE (A) and reconstituted HDL composed of apoA-I, DMPC, and 2 mol% Texas Red-DHPE (B) both show some association with cells. All images obtained at 10× magnification. ApoA-I, apolipoprotein A-I; DHPE, 1,2-dihexadecanoyl-sn-glycero-3-phosphoethanolamine, triethyl-ammonium salt; DMPC, 1,2-dimyristoyl-sn-glycero-3-phosphocholine.

a) reduced lateral mobilities in rHDL configuration as established by their effectively higher transition temperatures (36, 37) and *b*) the distribution of GM1 across multiple independent particles (the rHDL platform represents a significant steric impediment to a two-particle interaction). Third, there is significant evidence that suggests molecular flexibility of the receptor molecules within the membrane can influence binding interactions (38, 39). Phospholipids encased in reconstituted HDL display an elevated and broadened phase transition (36, 40) (also see supplementary data). It is possible that this increased membrane rigidity within the rHDL particle ensures the GM1 sugar moiety into a conformation that is more amenable to CTB binding. The reduced molecular fluidity, combined with the diminished clustering and cross-linking, should lead to more CTB-rHDL interactions and an increased association constant, both of which are evident in the data (Table 1).

Before discussing our measurements of toxin-cell interactions in the presence of GM1-laden rHDL decoys, we present control experiments designed to characterize interactions between rHDL and cells. Epifluorescence images reveal that fluorescently labeled rHDL and even vesicles sans GM1 (DMPC only), show significant interaction with RPE cells (**Fig. 4**). Of concern is the markedly higher fluorescence intensity in samples prepared with rHDL. Class B scavenger protein (a lipoprotein-binding protein) exists in the plasma membrane of RPE cell types and is thought to be responsible for intraretinal cholesterol transport (41–43). As high-density lipoprotein are known for their role in reverse cholesterol transport (44) (RCT), a physiological system designed to protect against atherosclerosis, it is not surprising to find interactions between RPE cells and rHDL. Whether rHDL are trafficked into the cells through an endocytotic process or simply bind to the cellular membrane is not discernable here. However, note that interactions between carrier rHDL and cells have a potential to compromise the protective potential of engineered lipoprotein, especially in cases where host cells contain lipoprotein-binding proteins.

By fluorescently labeling both toxin and protector, the location of each species after incubation can be identified. From the obtained images, rHDL samples show very little fluorescence after incubation and rinsing (**Fig. 5B**, D) relative to those prepared without any preventative measures (Fig. 5E). Of particular note is the ease with which toxin is removed from the cell's surroundings. Simple solution exchange after incubation is sufficient to prevent invasive binding while leaving the cells unharmed, as evidenced by the lack of fluorescence and persistence of healthy cell

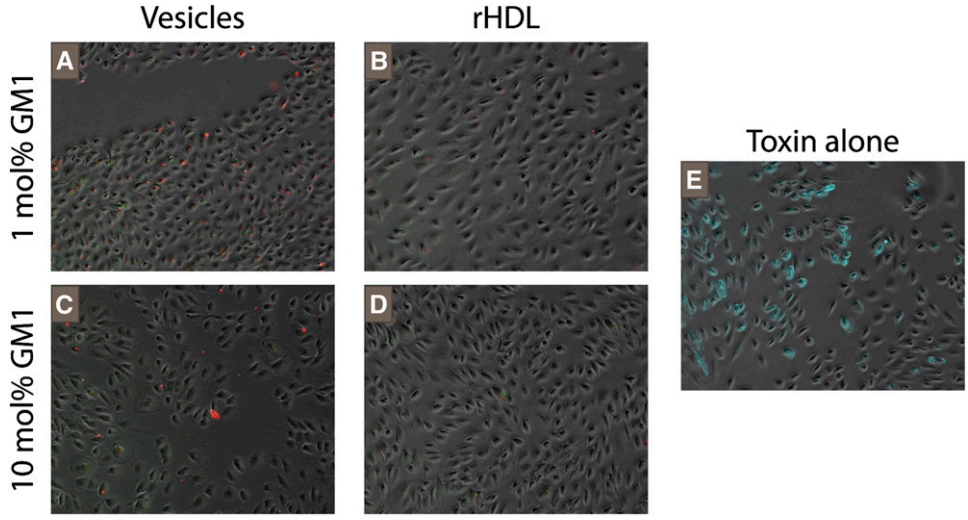

Fig. 5. Localization of toxin and decoy after incubation. Fluorescently-labeled lipid particles and cholera toxin B with human retinal pigment epithelial cells. Cells appear in gray with NBD-labeled rHDL in green, Alexa594-CTB in red, and FITC-CTB in cyan (E only). FITC-CTB was used for experiments involving only one fluorophore while Alexa594-CTB was used for experiments requiring multiple fluorophores to allow imaging of each probe on a separate channel. All images are contrast enhanced in a standardized fashion and captured at 10× magnification. CTB, cholera toxin subunit B; FITC, fluorescein-isothiocyanate; GM1, monosialotetrahexosylganglioside.

shape. When RPE cells expire, they detach from the petri dish, first taking on a more oval shape before releasing completely. After incubation, the cells retain their original shape, suggesting that they are not subject to any lethal stresses (specifically, rupture of the membrane due attachment of cholera toxin B). The opposite effect is seen with vesicle-based decoys where both green (phospholipid) and red (CTB) emission are apparent (Fig. 5A, C), indicating that these systems afford the cells little protection from toxin. This is true for both physiologically relevant concentrations of GM1 (1 mol%, Fig. 5A) and artificially inflated amounts (10 mol%, Fig. 5C). Thus, the control of clustering supersedes any advantage gained by adding additional receptors.

Remarkably, the interaction of rHDL with RPE cells (visible in Fig. 4) is not replicated when CTB and GM1-laden rHDL are added simultaneously (Fig. 5). The inclusion of both toxin and receptor strongly reduces cellular uptake and helps keep the cell free of not only toxin and rHDL but also lipoprotein-toxin complexes. This dramatic lowering of rHDL and CTB interactions with the RPE cells is intriguing. Control experiments performed without GM1 (see supplementary data) show that cholera does interact with cells when lipoprotein does not contain the toxin receptor; thus, the presence of GM1 is crucial to the inhibitory effect. At present, we cannot isolate the precise origin of this behavior. We speculate that once CTB binds to rHDL, the lipoprotein particle is no longer recognized by the lipoprotein receptor. From X-ray crystallography, the lateral area of the CTB pentamer is $\sim$30 nm^2 with a vertical height of roughly 3 nm (21). Once bound, the protein toxin represents a sizeable increase in the volume of the discoidal lipoprotein, whose average dimensions are a lateral area of 78.5 nm^2 and a height of 4.5 nm. From this comparison, it is not difficult to see how the large CTB molecule may present a significant steric hindrance to receptor binding. As for the improved effectiveness of rHDL samples over vesicles, we attribute this to the dissipation of clustering and cross-linking, which serves to enhance receptor-ligand affinity. This dissipation is a direct consequence of the much smaller lipoprotein size (10–20 nm diameter) relative to the signaling lipid rafts (50–500 nm diameter) of cellular membranes thought to house these receptors (45). Furthermore, vesicles composed of raft mixture (DOPC:SM:CH in a 1:1:1 ratio) display binding constants 34% lower than single-phase vesicles of identical GM1 concentration (Table 1). If GM1 is entirely localized within ordered domains, then the surface area accessible to ganglioside is severely restricted, causing an amplification of lateral aggregation. The observed 34% decrease lends further support to the theory of cluster-mediated binding and portends increased effectiveness of rHDL as a protective agent (25, 46).

Improved design and manipulation of artificial membrane-based constructs is important in the development of new research tools and therapeutic treatments. The reconstitution of lipoprotein from mixtures of apolipoprotein and phospholipid doped with membrane-bound receptors shows significant promise in addressing both of these demands. Utility as an investigative tool lies in the ability of rHDL to present receptors in a near-native environment and in a manner amenable to measurement with traditional biophysical techniques. As demonstrated here, the lipoprotein configuration enhances the effective interaction between toxin and receptor, due to the interplay between ligand-receptor affinity and the physical properties of the lipoprotein scaffold (namely, attenuation of receptor aggregation, cross-linking, and receptor conformation). In terms of a potential therapy, preliminary results from the incubation of GM1-laden rHDL with CTB and mammalian cells are encouraging. While our work describes application for a single ligand-receptor combination, we anticipate this platform could be of broad use in a variety of systems.

REFERENCES

1. Aderem, A., and R. Ulevitch. 2000. Toll-like receptors in the induction of the innate immune response. *Nature.* **406:** 782–787.
2. Gershoni, J. M. 2008. Molecular decoys: antidotes, therapeutics and immunomodulators. *Curr. Opin. Biotechnol.* **19:** 644–651.
3. Iwamori, M., K. Takamizawa, M. Momoeda, Y. Iwamori, and Y. Taketani. 2008. Gangliosides in human, cow and goat milk, and their abilities as to neutralization of cholera toxin and botulinum type A neurotoxin. *Glycoconj. J.* **25:** 675–683.
4. Newburg, D. S. 1996. Oligosaccharides and glycoconjugates in human milk: their role in host defense. *J. Mammary Gland Biol. Neoplasia.* **1:** 271–283.
5. Hamosh, M., J. A. Peterson, T. R. Henderson, C. D. Scallan, R. Kiwan, R. L. Ceriani, M. Armand, N. R. Mehta, and P. Hamosh. 1999. Protective function of human milk: the milk fat globule. *Semin. Perinatol.* **23:** 242–249.
6. Duncan, R. 2003. The dawning era of polymer therapeutics. *Nat. Rev. Drug Discov.* **2:** 347–360.
7. Jonas, A., and D. J. Krajnovich. 1977. Interaction of human and bovine A-1 apolipoproteins with L-alpha-dimyristoyl phosphadicylcholine and L-alpha-myristoyl lysophosphatidylcholine. *J. Biol. Chem.* **252:** 2194–2199.
8. Vinchurkar, M. S., D. A. Bricarello, J. O. Lagerstedt, J. P. Buban, H. Stahlberg, M. N. Oda, J. C. Voss, and A. N. Parikh. 2008. Bridging across length scales: multi-scale ordering of supported lipid bilayers via lipoprotein self-assembly and surface patterning. *J. Am. Chem. Soc.* **130:** 11164–11169.
9. Guo, L. S., R. L. Hamilton, J. Goerke, J. N. Weinstein, and R. J. Havel. 1980. Interaction of unilamellar liposomes with serum lipoproteins and apolipoproteins. *J. Lipid Res.* **21:** 993–1003.
10. Whorton, M. R., M. P. Bokoch, S. G. Rasmussen, B. Huang, R. N. Zare, B. Kobilka, and R. K. Sunahara. 2007. A monomeric G protein-coupled receptor isolated in a high-density lipoprotein particle efficiently activates its G protein. *Proc. Natl. Acad. Sci. USA.* **104:** 7682–7687.
11. Bayburt, T. H., A. J. Leitz, G. Xie, D. D. Oprian, and S. G. Sligar. 2007. Transducin activation by nanoscale lipid bilayers containing one and two rhodopsins. *J. Biol. Chem.* **282:** 14875–14881.
12. Bayburt, T. H., J. W. Carlson, and S. G. Sligar. 1998. Reconstitution and imaging of a membrane protein in a nanometer-size phospholipid bilayer. *J. Struct. Biol.* **123:** 37–44.
13. Baker, S. E., R. C. Hopkins, C. D. Blanchette, V. L. Walsworth, R. Sumbad, N. O. Fischer, E. A. Kuhn, M. Coleman, B. A. Chromy, S. E. Letant, et al. 2009. Hydrogen production by a hyperthermophilic membrane-bound hydrogenase in water-soluble nanolipoprotein particles. *J. Am. Chem. Soc.* **131:** 7508–7509.
14. Bayburt, T. H., and S. G. Sligar. 2003. Self-assembly of single integral membrane proteins into soluble nanoscale phospholipid bilayers. *Protein Sci.* **12:** 2476–2481.
15. Rensen, P. C., R. L. de Vrueh, J. Kuiper, M. K. Bijsterbosch, E. A. Biessen, and T. J. van Berkel. 2001. Recombinant lipoproteins: lipoprotein-like lipid particles for drug targeting. *Adv. Drug Deliv. Rev.* **47:** 251–276.
16. Feng, M., Q. Cai, X. Shi, H. Huang, P. Zhou, and X. Guo. 2008. Recombinant high-density lipoprotein complex as a targeting system of nosiheptide to liver cells. *J. Drug Target.* **16:** 502–508.

17. Newton, R. S., and B. R. Krause. 2002. HDL therapy for the acute treatment of atherosclerosis. *Atheroscler. Suppl.* **3:** 31–38.
18. Wu, J., M. Nantz, and M. Zern. 2002. Targeting hepatocytes for drug and gene delivery: emerging novel approaches and applications. *Front. Biosci.* **7:** d717–725.
19. Kader, A., and A. Pater. 2002. Loading anticancer drugs into HDL as well as LDL has little affect on properties of complexes and enhances cytotoxicity to human carcinoma cells. *J. Control. Release.* **80:** 29–44.
20. Brown, D., and E. London. 2000. Structure and function of sphingolipid- and cholesterol-rich membrane rafts. *J. Biol. Chem.* **275:** 17221–17224.
21. Merritt, E. A., S. Sarfaty, F. V. D. Akker, C. L'Hoir, J. A. Martial, and W. G. J. Hol. 1994. Crystal structure of cholera toxin B-pentamer bound to receptor G (M1) pentasaccharide. *Protein Sci.* **3:** 166–175.
22. Miller, C. E., J. Majewski, R. Faller, S. Satija, and T. L. Kuhl. 2004. Cholera toxin assault on lipid monolayers containing ganglioside GM1. *Biophys. J.* **86:** 3700–3708.
23. Sharom, F. J., and C. W. M. Grant. 1978. Model for ganglioside behavior in cell-membranes. *Biochim. Biophys. Acta.* **507:** 280–293.
24. Yuan, C., J. Furlong, P. Burgos, and L. J. Johnston. 2002. The size of lipid rafts: an atomic force microscopy study of ganglioside GM1 domains in sphingomyelin/DOPC/cholesterol membranes. *Biophys. J.* **82:** 2526–2535.
25. Shi, J., T. Yang, S. Kataoka, Y. Zhang, A. J. Diaz, and P. S. Cremer. 2007. GM (1) clustering inhibits cholera toxin binding in supported phospholipid membranes. *J. Am. Chem. Soc.* **129:** 5954–5961.
26. Ryan, R. O., T. M. Forte, and M. N. Oda. 2003. Optimized bacterial expression of human apolipoprotein AI. *Protein Expr. Purif.* **27:** 98–103.
27. Oda, M. N., T. M. Forte, R. O. Ryan, and J. C. Voss. 2003. Apolipoprotein A-I's C-terminal domain contains a lipid sensitive conformational trigger. *Nat. Struct. Biol.* **10:** 455–460.
28. Davenport, L., R. Dale, R. Bisby, and R. Cundall. 1985. Transverse location of the fluorescent probe 1, 6-diphenyl-1, 3, 5-hexatriene in model lipid bilayer membrane systems by resonance excitation energy transfer. *Biochemistry.* **24:** 4097–4108.
29. Lakowicz, J. R. 2006. Principles of Fluorescence Spectroscopy. Springer, New York.
30. Kong, H. J., T. Boontheekul, and D. J. Mooney. 2006. Quantifying the relation between adhesion ligand-receptor bond formation and cell phenotype. *Proc. Natl. Acad. Sci. USA.* **103:** 18534–18539.
31. Lauer, S., B. Goldstein, R. L. Nolan, and J. P. Nolan. 2002. Analysis of cholera toxin-ganglioside interactions by flow cytometry. *Biochemistry.* **41:** 1742–1751.
32. Lincoln, J. E., M. Boling, A. N. Parikh, Y. Yeh, D. G. Gilchrist, and L. S. Morse. 2006. Fas signaling induces raft coalescence that is blocked by cholesterol depletion in human RPE cells undergoing apoptosis. *Invest. Ophthalmol. Vis. Sci.* **47:** 2172–2178.
33. Yee, C. K., M. L. Amweg, and A. N. Parikh. 2004. Direct photochemical patterning and refunctionalization of supported phospholipid bilayers. *J. Am. Chem Soc.* **126:** 13962–13972.
34. Williams, T. L., and A. T. Jenkins. 2008. Measurement of the binding of cholera toxin to GM1 gangliosides on solid supported lipid bilayer vesicles and inhibition by europium (III) chloride. *J. Am. Chem. Soc.* **130:** 6438–6443.
35. Borch, J., F. Torta, S. Sligar, and P. Roepstorff. 2008. Nanodiscs for immobilization of lipid bilayers and membrane receptors: Kinetic analysis of cholera toxin binding to a glycolipid receptor. *Anal. Chem.* **80:** 6245–6252.
36. Tall, A. R., D. M. Small, R. J. Deckelbaum, and G. G. Shipley. 1977. Structure and thermodynamic properties of high density lipoprotein recombinants. *J. Biol. Chem.* **252:** 4701–4711.
37. Edwards, W. L., S. F. Bush, T. W. Mattingly, and K. H. Weisgraber. 1993. Raman spectroscopic study of boundary lipid in 1,2-dipalmitoylphosphatidylcholine/apolipoprotein A-I recombinants. *Spectrochim. Acta [A].* **49:** 2027–2038.
38. Burger, K., G. Gimpl, and F. Fahrenholz. 2000. Regulation of receptor function by cholesterol. *Cell. Mol. Life Sci.* **57:** 1577–1592.
39. Chachisvilis, M., Y. L. Zhang, and J. A. Frangos. 2006. G protein-coupled receptors sense fluid shear stress in endothelial cells. *Proc. Natl. Acad. Sci. USA.* **103:** 15463–15468.
40. Jonas, A., D. Krajnovich, and B. Patterson. 1977. Physical properties of isolated complexes of human and bovine AI apolipoproteins with L-alpha-dimyristoyl phosphatidylcholine. *J. Biol. Chem.* **252:** 2200–2205.
41. Duncan, K. G., K. R. Bailey, J. P. Kane, and D. M. Schwartz. 2002. Human retinal pigment epithelial cells express scavenger receptors BI and BII. *Biochem. Biophys. Res. Commun.* **292:** 1017–1022.
42. Hayes, K. C., S. Lindsey, Z. F. Stephan, and D. Brecker. 1989. Retinal pigment epithelium possesses both LDL and scavenger receptor activity. *Invest. Ophthalmol. Vis. Sci.* **30:** 225–232.
43. Tserentsoodol, N., N. Gordiyenko, I. Pascual, J. Lee, S. Fliesler, and I. Rodriguez. 2006. Intraretinal lipid transport is dependent on high density lipoprotein-like particles and class B scavenger receptors. *Mol. Vis.* **12:** 1319–1333.
44. Febbraio, M., D. P. Hajjar, and R. L. Silverstein. 2001. CD36: a class B scavenger receptor involved in angiogenesis, atherosclerosis, inflammation, and lipid metabolism. *J. Clin. Invest.* **108:** 785–791.
45. Simons, K., and E. Ikonen. 1997. Functional rafts in cell membranes. *Nature.* **387:** 569–572.
46. Thompson, T. E., M. Allietta, R. E. Brown, M. L. Johnson, and T. W. Tillack. 1985. Organization of ganglioside GM1 in phosphatidylcholine bilayers. *Biochim. Biophys. Acta.* **817:** 229–237.